Published in "Tree Physiology 27: 1229-1241, 2007"
which should be cited to refer to this work.

Fresh-wood bending: linking the mechanical and growth properties of a Norway spruce stem

TOR LUNDSTRÖM,[1–3] URS HEIZ,[1] MARKUS STOFFEL[3] and VERONIKA STÖCKLI[1]

[1] *WSL, Swiss Federal Institute for Snow and Avalanche Research SLF, 7260 Davos Dorf, Switzerland*

[2] *Corresponding author (t.lundstroem@slf.ch)*

[3] *Laboratory of Dendrogeomorphology, University of Fribourg, 1700 Fribourg, Switzerland*

Summary To provide data and methods for analyzing stem mechanics, we investigated bending, density and growth characteristics of 207 specimens of fresh wood from different heights and radial positions of the stem of one mature Norway spruce (*Picea abies* L. Karst.) tree. From the shape of each stress–strain curve, which was calculated from bending tests that accounted for shear deformation, we determined the modulus of elasticity (MOE), the modulus of rupture (MOR), the completeness of the material, an idealized stress–strain curve and the work involved in bending. In general, all mechanical properties increased with distance from the pith, with values in the ranges of 5.7–18 GPa for MOE, 23–90 MPa for MOR and 370–630 and 430–1100 kg m^{-3} for dry and fresh wood densities, respectively. The first three properties generally decreased with stem height, whereas fresh wood density increased. Multiple regression equations were calculated, relating MOR, MOE and dry wood density to growth properties. We applied these equations to the growth of the entire stem and considered the annual rings as superimposed cylindrical shells, resulting in stem-section values of MOE, MOR and dry and fresh densities as a function of stem height and cambial age. The standing tree exhibits an inner stem structure that is well designed for bending, especially at a mature stage.

Keywords: annual ring width, bending mechanics, bulk density, heartwood, knottiness, latewood, sapwood, stem growth, water content.

Introduction

An important factor determining the stability of trees is the way in which stems bend under the pressure of the wind or when impacted by rock falls or avalanches. To understand and predict how stems bend, information about the material properties of living stems is required. In particular, information is needed concerning the relationships between properties of growth, which are affected by forest management practices, and properties of bending mechanics.

For dry and manufactured wood, the effects of growth on mechanics are relatively well understood, as they are relevant to the wood and paper industry. Research on the effects of thinning regimes, fertilization and genetic plant manipulation on mechanical wood properties has greatly contributed to this knowledge (Kollmann 1968, Schmidt-Vogt 1991, Niemz 1993, Lindstrom 1996, 1997, Saren et al. 2001). In brief, because the properties of tracheids correlate with age and properties of annual rings (Dinwoodie 1961, Fioravanti 2001), the most important variables to consider when estimating the mechanical properties of clear dry wood of conifers are the annual ring width, or the percentage of latewood, and tree age (Deresse and Shepard 1999, Sirviö 2001).

An increase in the water content (u) of fresh wood (abbreviations and their definitions are listed in the Appendix) lowers strength and stiffness, and generally reduces the modulus of elasticity (MOE) and the modulus of rupture (MOR) by a magnitude that depends on dry wood density (Dinwoodie 2000), although low-quality timber seems to be less affected (e.g., fir; Madsen 1975). An increase in u also lowers the longitudinal shear modulus (G) and resistance (τ), which affect MOE and MOR. The negative effect of an increase in u from the usual value of 12% to the point of fiber saturation (about 50%) is, in order of importance: MOR, τ, G and MOE (Kollmann 1968, Green et al. 1999), whereas an increase in u above about 50% has no significant effect on any of these properties. However, high u values affect the bulk density of fresh wood and thus the mass of the living stem. Stem mass has a significant influence on the root–soil moment and the stem stresses in a leaning tree (Neild and Wood 1999), as well as on tree structural dynamics when the stem is subjected to acceleration (Milne 1991, Dorren and Berger 2006). For healthy conifer wood, the change in u that occurs in the transition from sapwood to heartwood as a result of torus closure of tracheids is the only factor that influences the mechanical properties of wood once the differentiation of cambial xylem initials is complete (Siau 1995).

The presence of knots, whether dead or alive, greatly reduces resistance to tension, but does not significantly affect

compression or shear strength (Kollmann 1968). In timber from *Picea abies* L. Karst. and *Pinus sylvestris* L., knots can lower MOR by up to 75% (Kucera 1973), but their influence on deformation and resistance is lower in intact stems than in sawn-wood products (Green et al. 1999). Kucera (1973) also showed that dead and live knots reduce bending resistance to about the same extent, although the Nordic timber-grading rules (FSS 1997) penalize, to some extent, dead and unsound knots compared with live knots. In general, knots also appear to slightly reduce the MOE of dry wood (Kollmann 1968, Dinwoodie 2000).

The inner-stem structure of Norway spruce displays gradients in annual ring width and percentage of latewood (www.ncdc.noaa.gov/paleo/treering.html). Although a multitude of growth patterns can be found depending on growth conditions, ring width generally decreases and the percentage of latewood increases from the pith toward the bark, with the trends reversing with tree height (Trendelenburg and Mayer-Wegelin 1955). The radial and longitudinal trends in growth pattern are more evident in mature trees, with the exception of suppressed trees (Deresse and Shepard 1999). Water content also exhibits gradients within the stem. In Norway spruce, heartwood water content ranges between 30 and 50%, whereas sapwood displays a season-independent water content that is commonly above 150% in early spring and below 100% in late summer (Trendelenburg and Mayer-Wegelin 1955, Schmidt-Vogt 1991). The presence of knots within the stem results from the self-pruning of dead branches at the crown base. The relative height at which self-pruning occurs increases as trees compete for light, resulting in radial and longitudinal gradients in knot frequency (Ikonen et al. 2003).

Analysis of wood bending includes deformation caused by longitudinal tension, compression and shearing (Newlin and Trayer 1956), and related failure mechanisms. Tests on clear, dry and fresh wood show that elasticity along the grain in tension equals that in compression, but that tension failure stresses are higher than those in compression (Natterer et al. 2000). Because of differences in failure stresses and gradients in the growth pattern and local material heterogeneities, a gradual redistribution of compression, tension and shear stresses occurs as the bending load increases (Kollmann 1968). This redistribution is marked for wood with continuous wood fibers, as was shown in studies of dry logs (Adjanohoun et al. 1998, Natterer et al. 2000). Compared with sawn logs, intact logs have a 10% higher MOE, on average, and a 15–25% higher MOR (Natterer and Sandoz 1997).

Turning living tree stems into dry timber, and especially into clear wood, has several effects on material properties related to bending. The overall goal of this study was to analyze stem mechanics. Specific objectives were to: (1) relate dry and fresh wood density and bending properties of a stem with radial and vertical position in the stem; (2) develop statistical regression models linking the mechanical properties of stem wood with radial growth properties; and (3) apply the regression models based on the data in (1) to the entire stem to determine stem-section values of dry and fresh density, MOE and MOR as a function of height and cambial age.

Materials and methods

Tree and test samples

We investigated bending mechanics, density and growth properties of the fresh stem wood of one mature, co-dominant Norway spruce tree growing at an elevation of 460 m near Zürich in Switzerland, on a dystric Cambisol (FAO 1998), in a mixed forest stand (Lundström et al. 2007). The selected tree was representative of other Norway spruce trees in the stand. Characteristics of the test tree were: diameter at breast height (DBH), 400 mm; cambial age (AGE) at breast height, 100 years; total height (H), 35.0 m; length of the green crown relative to H, 0.42; and bark thickness at breast height relative to DBH, 6%. The tree was straight and apparently healthy.

The test Norway spruce tree was felled in mid-November and the stem transported to the laboratory where it was placed outside on level ground in the shade. The next day, stem diameter and bark thickness were measured at 1-m intervals. The stem was then subjected to five successive cutting steps (cf. Figure 1): (1) three 3-m-long log sections (each comprising log sections T3 + T2 + T1), with their base:top at stem heights of 0.7:3.7, 10.1:13.1 and 19.2:22.2 m, respectively; (2) three shorter log sections (T1, T2, and T3) 0.5, 0.9 and 1.6 m in length, respectively, with the section center at relative stem heights (z_{rel}) = z/H of 0.04 (T3), 0.08 (T2) and 0.10 (T1) of the first 3-m log, 0.31 (T3), 0.35 (T2) and 0.37 (T1) of the second, and 0.57 (T3), 0.61 (T2) and 0.63 (T1) of the third 3-m log; (3) quarter sections (A, B, C and D); (4) planks (I, II, ….VI); and (5) bending specimens, ranging from bark to pith (1, 2, …8).

The bending specimens were 20 × 20 × 360 mm (127 pieces cut from the three log sections denoted T1), 40 × 40 × 720 mm (61, T2) and 80 × 80 × 1440 mm (19, T3), with a total of 113 bending specimens from the heartwood and 94 from the sapwood. The transition between the water-conducting sapwood and the heartwood was set to where there was a steep radial in-

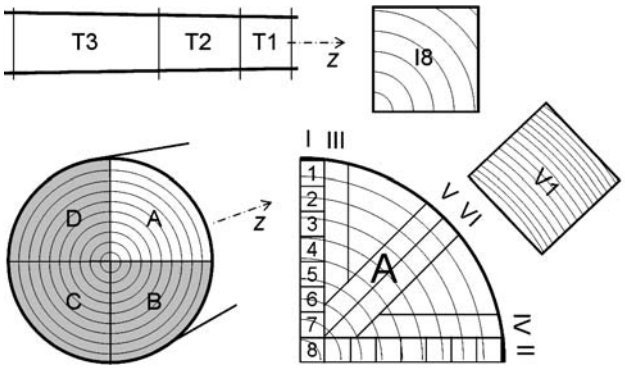

Figure 1. To obtain specimens for bending, each of three 3-m-long logs (top, one 3-m log) cut from the Norway spruce stem was sawn into three shorter sections (T1–3). These shorter sections were then cut into quarter sections (A–D, left), planks (I–VI, right) and finally into bending specimens with square cross sections (1–8, right, with examples shown for bending speciments, I8 and VI). Annual rings are displayed schematically in the cross sections, with light gray circles (left) and circle sectors (right).

crease in water content. Altogether 207 bending specimens were obtained. For each specimen, annual ring width (RW) and percentage of latewood (LW) were measured with a caliper and averaged over the cross section. The specimens were grouped into four categories according to the approximate orientation of the annual rings, with Cut = 1 corresponding to almost straight rings, Cut = 4 to rings resembling a quarter of a circle, and Cut = 2 and 3 to intermediate patterns. This grouping depended on the cutting scheme position of the specimen. For example, the specimens from the inner heartwood were grouped in Category 4, and the ones from the outer sapwood in Category 1 (cf. Figure 1). In addition to the bending specimens, stem discs were cut from z_{rel} = 0.0085 (i.e., at z = 0.30 m), 0.75, 0.90 and 0.99 to analyze radial growth.

Knot frequency was described by a three-number classification. The first number refers to knottiness Q (SIA 2003) of the cross section, which is the ratio between the sum of diameters of knots on the compression- (upper) and tension- (lower) side of the test specimen, along the middle 150 mm of the span, and twice the specimen width. The second and third numbers were calculated accordingly, but refer specifically to the knots on the tension- (t) and the compression- (c) side of the specimen, Q_t and Q_c, respectively. Although most knots were living, no distinction was made between dead and live knots. Because the annual ring curvature was generally small compared with specimen size, the frequently used Knot Area Ratio (KAR, SIA 2003) was less than or equal to 2Q. Wood defects other than knots were not observed among the test specimens.

Tests and investigations

The specimens were tested in 3- and 4-point bending (187 and 20 specimens), according to the German industry code, DIN 52186 (DIN (1992) includes all the mentioned DIN codes), with an exception made for their water content u. For this purpose, we used a hydraulic vertical press D-200-VS 91 connected to a data logger PK-SRG-5000 124 (Walter+Bai AG, Löhningen, Switzerland). The load was applied with a constant deflection rate so that the maximum force was obtained within 90 ± 30 s. With load and deflection sampled at 1 Hz, the tests were continued until complete failure of the specimen occurred. After testing, the wood samples were cut close to the failure zone to analyze u and the dry and fresh wood density ($\rho 0$, ρU) according to DIN 52182 and DIN 52183. To calculate $\rho 0$, we used the dry volume and the wet mass, and corrected for tree volumetric shrinkage with the factor 1.10 (Kollmann 1968). The bending tests and the determinations of u were completed within one day of specimen cutting and one week of tree felling.

Mechanical analysis

All data related to bending mechanics, such as MOE and MOR, were based on the complete curves for bending stress (σ) as a function of bending strain (ε), from no load up to maximum load and then until the load returned to near zero. To obtain these curves, we followed five steps (Table 1) and used Equation 1:

$$E = \frac{F}{s}\left(\frac{C_1}{48I} + C_2\right);\ I = \frac{bh^3}{12}$$
$$C_1 = \frac{1}{2}(2L^3 - 3LL_F{}^2 - L_F{}^3);\ C_1 = L^3 \quad (1)$$
$$C_2 = \beta\left(\frac{E}{G}\right)'\frac{L}{bh}$$

where F is the applied force (N), L, b and h are the length, width and height of the bending specimens (mm), s is the mid-span deflection (Mm), L_F is the distance between support and force application (mm), C_1 is a length factor that equals L^3 in 3-point bending, C_2 is a correction factor for shear deformation, β is a load coefficient that equals 8/27 and 16/81 in 3- and 4-point bending, respectively (Newlin and Trayer 1956), and $(E/G)'$ is an estimated relationship between the elasticity in bending (E) and shear (G) along the grain. For sawn wood of Norway spruce with a density = 400–600 kg m^{-3}, and u = 12%, E/G has a mean of 18 and is about 21 for green wood (u > 50%: Kollmann 1968), which is the value that we adopted for $(E/G)'$. The mass of the bending specimens contributed less than 0.2% to MOR and was therefore omitted from the analysis. Except for the analysis of MOE (Table 1), $\sigma(\varepsilon)$ is used throughout this study.

We also established characteristic $\sigma(\varepsilon)$ curves, where each was the mean stress–strain curve for a specific group of bending specimens. A distinction was made between three groups of mean relative heights 0.10 (1), 0.37 (2) and 0.63 (3), and between two radial ranges, the inner heartwood (IH) and the sapwood (S). The outer heartwood (OH), with properties between the S- and IH-groups, was analyzed only individually. Each of the six groups included between 18 and 32 $\sigma(\varepsilon)$ curves from the small- and medium-sized bending specimens. The

Table 1. Successive steps in the bending mechanics analysis. Abbreviations: σ, bending stress; MOR, modulus of rupture; and MOE, modulus of elasticity.

Step	Description
1	Calculation of σ due to the applied force (DIN 52 186). The maximum σ, independent of type of failure, corresponds to MOR.
2	Calculation of the elasticity in bending (E) due to the applied force (DIN 52 186), corrected for shear deformation (Equation 1).
3	Combination of results from steps 1 and 2 into the bending strain $\varepsilon_E = \sigma/E$ and computation of $\sigma(\varepsilon_E)$. As E is corrected for shear deformation, ε_E is the strain as it would be under pure bending conditions.
4	Definition of MOE as $E(\varepsilon_E)_{0.4MOR}$, the gradient of the straight line between $\sigma(\varepsilon_E) = 0$ and $\sigma(\varepsilon_E) = 0.4$MOR. The initial deformations at supports are not included in the ε_E data.
5	Calculation of $\sigma(\varepsilon)$: ε is the apparent strain from no load until the end of the test, thus with no correction for shear deformation (ε is slightly larger than ε_E).

stress–strain curves obtained were further described with simplified ideal elastic–ideal plastic curves. The break point $(\sigma,\varepsilon) = (\varepsilon_{el\text{-}pl}, MOR \cdot \alpha_{el\text{-}pl})$ between ideal elastic and ideal plastic deformation was conditioned by an equal amount of total work absorbed by the bent member up to σ = MOR, compared with the original $\sigma(\varepsilon)$ curve.

The absorbed bending work (W) (Equation 2) and the completeness of the material (η) (Equation 3) were both calculated from the load–deflection curve $F(s)$:

$$W = \int_s F(s)ds \tag{2}$$

$$\eta = \frac{W_{MOR}}{F_{max} s_{MOR}} \tag{3}$$

where F_{max} is the maximum applied force (N), s_{MOR} is the value of s at MOR (mm) and W_{MOR} is the work developed up to MOR (N m). The values of total work (W_{tot}) absorbed by the bending specimen during the entire bending test were compared for specimens of the same size. To compare with work absorbed by specimens of other dimensions (e.g., Märki et al. 2005), W_{tot} was divided by the volume (V) of the specimen within the span. For calculations of W/V, only the specimens tested in 3-point bending were included because a larger part of the bending specimen is activated in bending stress in 4-point bending than in 3-point bending, which mobilizes more W/V in 4-point bending. Moreover, work was also expressed in terms of σ integrated with respect to ε, as denoted by $\int \sigma(\varepsilon)d\varepsilon$. This number characterizes the material and is independent of the set-up and cross section of the test, just like η. We used Matlab 7.0 (MathWorks) for all mechanics analyses.

Statistical analysis

The statistical relationships within and between the growth characteristics and mechanical properties were explored with S-Plus 2000 (Insightful Corporation). We first applied the pair-wise test between variables to detect their possible transformation and then performed forward and backward stepwise linear regression of the model response variables described by the explanatory variables.

To qualitatively rank the regression models, we used the Akaike Information Criterion AIC (Sakamoto et al. 1986) and the Mallows's Cp statistic (Daniel et al. 1980), where low absolute values of AIC and Cp reflect high quality. The quality of model i was expressed as $AIC_{rel,i} = (1/AIC_i)/(1/AIC_1)$ and $Cp_{rel,i} = (1/Cp_i)/(1/Cp_1)$, where i = 1 is the highest ranked model. We also calculated the R^2 of each model, but as this overestimates the quality of multivariate regression models of correlated variables, it was given third priority in the model ranking. We know of no mathematically correct and straightforward method to calculate the amount of the total variance that each X_j (j = 1, 2,… n – 1, n) explains in a multivariate model of correlated variables (our case). Therefore, to rank the importance of each X_j for its contribution to Y, we used the difference in Cp value between the full, highest ranked model and the model lacking the X_j ("$-X_j$", Equation 4):

$$+Cp_j = \sum_{j=1}^{n-1} \frac{Cp(Model - X_j) - Cp(Model)}{Cp(Model)} \tag{4}$$

The effect of each X_j on Y was expressed by the standardized regression coefficient of X_j, $\boldsymbol{a_j} = a_j \cdot SE(X_j)/SE(Y)$. Because the investigated mechanical properties were obtained per tested specimen, the growth characteristics needed to be averaged for each bending specimen. For this reason, the large- and medium-sized specimens were less useful for describing the statistical relationships between the properties of growth and mechanics than the small specimens. Consequently, we used only the small specimens.

Application of statistical relationships to the mechanical properties of the entire tree stem

The growth data between pith and bark at seven values of z_{rel} were interpolated radially every millimeter and longitudinally every percent of tree height (piecewise cubic interpolation). The growth data at z_{rel} = 0.10, 0.37 and 0.63 originated from the 188 small- and medium-sized specimens, and those at z_{rel} = 0.0085, 0.75, 0.90 and 0.99 from stem discs sampled at these heights. Data on u were not obtained at the latter heights and originate from neighboring Norway spruce trees with a growth pattern similar to that of our test tree at z_{rel} = 0.10, 0.37 and 0.63 (unpublished SLF). Application of RW, u and Q to the regression equations resulted in $\rho 0$, ρU, MOE and MOR within the entire stem. The four mechanical properties were then calculated for the stem section as a function of stem height and AGE at breast height, with the relative distribution of u approximated so as not to vary with AGE (Trendelenburg and Mayer-Wegelin 1955, Schmidt-Vogt 1991).

To calculate $MOE_{section}$ (Equation 5), we used cylindrical shells ranging radially (x, which due to the circular shape, equals r) from pith (j = 1) to bark (j = n) every mm and longitudinally (z) from stem base (i = 1) to tree top (i = 101) every percent of tree height.

$$MOE_{section,i} = \frac{1}{x_n^4} \sum_{j=1}^{n} MOE(x)_{i,j}(x_{i,j+1}^4 - x_{i,j}^4) \tag{5}$$

The calculation of $MOR_{section}$ assumes, in principle, that $\sigma(x)$ as $MOR_{section}$ is reached, is known. In default of this knowledge, and ongoing from the strain–stress distribution of dry timber as its cross section reaches MOR (Kollmann 1968), we used two equations to calculate $MOR_{section}$. The first (Equation 6) applies a linear increase in longitudinal strain from pith to bark, with a gradient governed by the strain at MOR for the cylindrical shell at the radial distance of $\kappa_1 x_n$, where κ_1, is a factor between 0 and 1 (method of linear strain).

$$MOR_{section,i} = \frac{1}{x_n^3} \sum_{j=1}^{n} \sigma(\varepsilon, x, \kappa_1)_{i,j}(x_{i,j+1}^3 - x_{i,j}^3) \tag{6}$$

Unlike this first approach, which requires knowledge of $\sigma(\varepsilon,x)$, the second approach (Equation 7) is simpler. It applies a degree of exploitation $B(\kappa_2)$ of MOR_j, where $B(\kappa_2)$ is an array that increases from 0 to 1 between $x = 0$ and $x = \kappa_2 x_n$ and then remains constant, at a value of 1, between $x = \kappa_2 x_n$ and x_n (method of scaled MOR). Referring, once again, to dry timber, we set both κ_1 and κ_2 equal to 0.85.

$$MOR_{section,\,i} = \frac{1}{x_n^3}\sum_{j=1}^{n} MOR(x)_{i,\,j} B(\kappa_2)_{i,\,j}\left(x_{i,\,j+1}^3 - x_{i,\,j}^3\right) \quad (7)$$

Finally, the calculations of $\rho 0_{section}$ and $\rho U_{section}$ were simply quadratic summations of dry and fresh wood densities from the pith to the bark (Equation 8).

$$\rho_{section,\,i} = \frac{1}{x_n^2}\sum_{j=1}^{n} \rho(x)_{i,\,j}\left(x_{i,\,j+1}^2 - x_{i,\,j}^2\right) \quad (8)$$

Results

Failure mechanisms and behavior of bending stress–strain

The failure mechanism of the fresh bending specimen started with the wood fibers buckling on the compression side, followed by the fibers tearing apart on the tension side. The latter often occurred close to knots if they were present in the mid-span of the specimen. No signs of shear failure were observed.

The complete $\sigma(\varepsilon)$ curves showed five general features depending on the radial and height position in the stem (Figure 2A and Table 2). First, all bending specimens, independent of height or radial position, displayed a non-negligible remaining resistance beyond the strain at MOR, ε_{MOR}. Second, generally, W_{tot} increased from the IH-wood to the S-wood. Third, W_{tot}, MOE and MOR of the S-wood were almost identical at stem heights 1 and 2, but lower at height 3, and the W_{tot} of the IH-wood decreased with increasing stem height, whereas its MOE and MOR changed little. Fourth, although $\sigma(\varepsilon)$ differed in magnitude depending on height or radial position, $\sigma(\varepsilon)$/MOR curves were similar in shape until ε_{MOR} was reached (Figure 2B). Fifth, beyond ε_{MOR}, $\sigma(\varepsilon)$ displayed a more abrupt drop in the IH-wood compared with the S-wood.

Table 2 shows that MOE and MOR were both about 60% higher and that W_{tot}/V is twice as large for the S-wood than for the IH-wood. It was also apparent that the characteristics of the simplified stress–strain curves were independent of the position within the stem. At the individual specimen level, the IH-wood displayed a step-wise decrease of σ after MOR (Figure 2C). Generally, this stair-case pattern smoothed gradually toward the bark. The SEs of the six mean $\sigma(\varepsilon)$/MOR curves (Figure 2B) were larger after MOR and for the IH-wood than before MOR and the S-wood (Table 2). There was a weak general increase in ε_{MOR} with MOR (Figure 2C and Table 3).

Not accounting for shear deformation in the 3- and 4-point bending tests led to underestimates of MOE of about 11 and 6%, respectively. Apart from this and W_{tot}/V, there were no significant differences in bending properties between the 3- and 4-point bending tests.

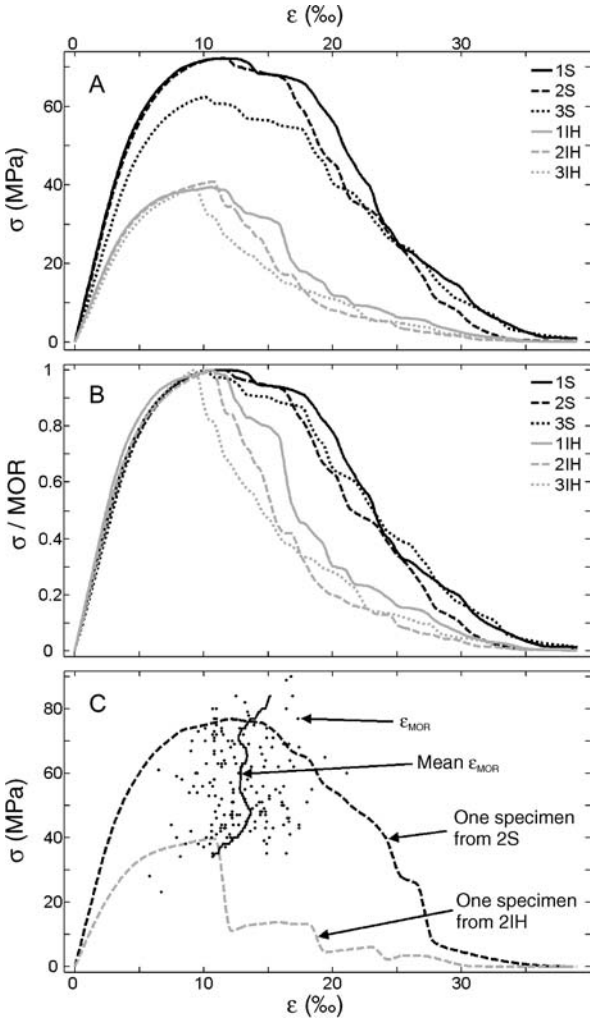

Figure 2. (A) Mean bending stress (σ) as a function of bending strain (ε). (B) IH refers to the inner heartwood, S to the sapwood, and 1, 2 and 3 to relative tree heights 0.10, 0.37 and 0.63, respectively. The $\sigma(\varepsilon)$/modulus of rupture (MOR) curves are similar in shape until the strain reaches MOR (ε_{MOR}), but not when the strain exceeds ε_{MOR}. This is evident in the IH-wood, especially in individual specimens (C). Values of ε_{MOR} (points) tended to increase with MOR (continuous line, mean ε_{MOR} = ε_{MOR} smoothed with the loess algorithm, Matlab).

Growth and mechanics measured across the stem

The measured properties of growth displayed characteristic patterns from the pith to the bark: RW decreased, whereas LW and *u* generally increased, with values in the range of 0.5–6.5 mm for RW, 0.10–0.71 for LW and 26–145% for *u*. Knottiness followed a Gaussian curve, with its maxima further from the bark at the stem base than higher up the stem. Values of *Q* ranged from 0 to 0.9 (apart from one specimen with Q = 1.8) and averaged 0.12. The most obvious dependency on tree

Table 2. Parameters obtained from the curves of bending stress–strain σ(ε) for groups of specimens from different positions in the stem. 1, 2 and 3 denote the relative stem heights 0.10, 0.37 and 0.63, S the sapwood and IH the inner heartwood. For example, 1S refers to the average stress–strain curve for sapwood at the relative height 0.10 and S to the average curve for all sapwood. Abbreviations: MOR, modulus of rupture, and MOE, modulus of elasticity.

Sample group	ε[1]				SE(σ(ε)/MOR)		α_{el-pl}[2] (%)	η[3]	W_{MOR}			MOR (MPa)	MOE (GPa)
	el (‰)	el–pl	MOR	max	$<\varepsilon_{MOR}$ (%)	$>\varepsilon_{MOR}$			$\int\sigma(\varepsilon)\,d\varepsilon$[4] (MPa)	/V[5] (KPa)	/W_{tot}[6] (%)		
1S	2.1	5.0	12	38	2	9	92	72	0.62	71	42	72.9	15.1
2S	2.1	5.2	14	35	4	9	93	74	0.68	77	52	70.4	14.2
3S	2.4	5.6	13	37	2	10	93	71	0.53	61	44	62.9	11.8
S	2.2	5.3	13	37	3	10	92	72	0.61	70	46	68.8	13.7
1IH	2.1	4.8	14	31	8	13	92	76	0.46	63	67	44.5	9.6
2IH	2.2	5.1	14	31	3	10	92	75	0.44	61	76	42.8	8.5
3IH	2.4	5.2	11	31	4	14	90	69	0.31	41	63	40.9	8.0
IH	2.2	5.0	13	31	5	12	91	73	0.40	55	69	42.7	8.7
All	2.2	5.1	13	34	4	11	92	73	0.51	62	57	55.7	11.2

[1] Bending strain at 0.4MOR (el), at the break point for the idealized σ(ε)-curve between ideal elastic and ideal plastic behavior (el–pl), at MOR and as σ returned to a value below 0.5 MPa (max).
[2] Stress level of plasticity for the idealized stress–strain curve, expressed as a fraction of MOR.
[3] Completeness of the material in bending (Equation 3).
[4] Integration of σ(ε) up to MOR, i.e., area under σ(ε) curve.
[5] Work absorbed in bending up to MOR, relative to the volume *V* within the span of the specimen.
[6] Total work absorbed in bending, i.e., up to ε_{max}.

height was the increase in *u*. The mechanical properties followed similar patterns to the growth characteristics across and along the stem. All mechanical properties generally increased with distance from the pith, with MOR in the range 23–90 MPa, MOE 5.7–18.1 GPa, W_{tot}/V 35–219 kPa, W_{MOR}/V 20–128 kPa, and ρ0 and ρU in the ranges 370–630 and 430–1100 kg m^{-3}, respectively. Except for *W*, all general tendencies or means of measured values are shown in Figures 3 and 4.

Relationships between the properties of mechanics and growth

As expected, several of the 13 variables of growth and mechanics were strongly correlated (Table 4). This resulted in regression models for the response variables ρ0, MOR and MOE, with six or less significant variables. Altogether 40 useful models describing ρ0 (9), MOR (20) and MOE (11) were obtained. Nine of these models are described in Tables 5–7.

Among the three response variables, ρ0 was modeled with

Table 3. Regression models for the strain (ε) at the modulus of rupture (MOR), $\varepsilon MOR_i = \sum_{j=1}^{n} a_j X_j$. Variable and intercept coefficients a_j, and standardized variable coefficient $\boldsymbol{a_j}$. The models ($\varepsilon MOR_{1,2}$) and the model variables X_j are listed top down according to the ranking and contribution to the model, respectively. The degrees of freedom are 122. Significance: *, $P < 0.05$; **, $P < 0.01$; and ***, $P < 0.001$.

Model				Variables				
i	AIC_{rel}[1]	Cp_{rel}[1]	R^2	X_j	a_j	SE(a_j)	$\boldsymbol{a_j}$	+Cp_j[2]
1	1.00	1.00	0.50	log(ρ0)	−2.92E−02 ***	2.89E−03	−2.05	0.47
				MOR	3.77E−04 ***	3.78E−05	2.29	0.46
				MOE	−3.25E−07 **	1.01E−07	−0.38	0.04
				z_{rel}	−2.23E−03 **	7.68E−04	−0.20	0.03
				Intercept	1.76E−01 ***	1.61E−02		
2	0.71	0.40	0.30	MOR	1.22E−04 ***	2.25E−05	0.64	0.47
				u	−4.12E−05 ***	7.89E−06	−0.47	0.44
				log(RW)	1.32E−03 *	5.44E−04	0.33	0.07
				Q	−1.59E−03 *	8.42E−04	−0.12	0.03
				Intercept	7.59E−03 ***	1.71E−03		

[1] $AIC_{rel,i} = (1/AIC_i)/(1/AIC_1)$ and $Cp_{rel,i} = (1/Cp_i)/(1/Cp_1)$, where $AIC_1 = -1254$ and $Cp_1 = 3.77E-04$ are the criteria of the highest ranked model (εMOR_1) and i = 1, 2 refers to each of the two models.
[2] +Cp_j is the relative contribution of each variable to Cp of the model (Equation 4).

Table 4. Correlation coefficients between variables: modulus of rupture (MOR), modulus of elasticity (MOE), annual ring width (RW), latewood portion (LW), dry wood density (ρ0), water content (u), squared knottiness of the specimen section (Q^2), on the compression (Q_c^2) and on the tension side (Q_t^2) of the specimen, cambial age (AGE) and distance (r) counted from pith toward bark, cutting mode (Cut), describing the annual ring curvature of the sample crosssection, and the relative tree height (z_{rel}).

	MOR	MOE	log(RW)	LW	ρ0	u	Q^2	Q_c^2	Q_t^2	AGE	r	Cut
MOE	0.82											
log(RW)	−0.87	−0.77										
LW	0.84	0.68	−0.77									
ρ0	0.95	0.75	−0.92	0.80								
u	0.63	0.43	−0.74	0.54	0.72							
Q^2	−0.27	−0.27	0.17	−0.18	−0.15	−0.07						
Q_c^2	−0.16	−0.21	0.10	−0.11	−0.07	−0.01	0.79					
Q_t^2	−0.27	−0.21	0.18	−0.18	−0.18	−0.12	0.66	0.07				
AGE	0.88	0.82	−0.84	0.73	0.88	0.50	−0.24	−0.18	−0.20			
r	0.84	0.80	−0.77	0.71	0.79	0.38	−0.30	−0.24	−0.22	0.96		
Cut	−0.58	−0.47	0.52	−0.45	−0.55	−0.33	0.07	−0.03	0.15	−0.61	−0.62	
z_{rel}	−0.11	−0.26	0.00	−0.05	−0.06	0.48	−0.02	0.02	−0.04	−0.35	−0.36	0.23

the highest quality, followed by MOR and then MOE. The variable ρ0 was strongly related to RW and LW (Table 5), and MOR was best described by ρ0 (Table 6). Although Q_t reduced MOR about twice as much as did Q_c, the overall frequency of knots was low, so knottiness contributed little to the quality of the models. The exclusion of ρ0 in the starting set of variables involved log(RW) in the models describing MOR (MOR_{2-4}) because ρ0 and log(RW) were strongly correlated. Excluding ρ0 also suggested models including AGE. However, these models contained additional variables that improved model quality little. Although Cut (= 1, 2, 3 or 4) tended to reduce MOR = –18.9log(Cut) + 67.5 (R^2 = 0.35, both coefficients $P < 0.001$), its influence was weak because of the strong correlation with other variables in the multivariate models (Table 4) and the presence of mainly straight annual rings (Cut = 1 or 2). The models describing MOE included log(RW), u and ρ0 (Table 7). Although MOE was also reduced by Q_c (P = 0.10), Cut and AGE, their impact on MOE, like that of MOR, was weak (for the same reasons).

Growth and mechanics within the stem

The growth properties interpolated within the entire stem (Figure 3) were applied to the regression models describing mechanical properties within the stem (Figure 4). These two property groups display some general features. For example, the zone between the IH-wood and the S-wood constitutes a transition for all properties of growth and mechanics except for Q. Between z_{rel} = 0.1 and 0.5, Q appears to be primarily influenced by the location of the lower part of the crown, changing from z_{rel} = 0.1 at AGE = 10 years to z_{rel} = 0.5 at 35 years, after which it increased little with height with increasing AGE.

Mechanics of the stem section

All mechanical properties of the stem section (Figure 5) decreased with stem height, except for $\rho U_{section}$, which increased. Within the stem section covered by the crown, $MOR_{section}$, and especially $MOE_{section}$, decreased with increasing height. At the buttressed stem base, the large RW in the outermost stem section reduced $MOR_{section}$ and $MOE_{section}$. At AGE = 100 years at breast height, the section values of MOR (Figure 5B) obtained by the linear strain method (Equation 6) were between 8 and 12% lower than those obtained by the scaled MOR method (Equation 7). These differences, which were largest at the stem base and in the crown, resulted from the different radial

Table 5. Regression models for the dry wood density ($\rho 0_i$). The models ($\rho 0_{1-2}$) and the model variables (X_j) are listed top down according to the ranking and contribution to the model, respectively. The minimum degrees of freedom (for $\rho 0_1$) are 124. Notations and footnotes are further explained in Table 3.

Model				Variables				
i	AIC_{rel}[1]	Cp_{rel}[1]	R^2	X_j	a_j	SE(a_j)	$\boldsymbol{a_j}$	$+Cp_j$[2]
1	1.00	1.00	0.87	log(RW)	−8.59E+01 ***	5.81E+00	−2.06	0.93
				LW	1.48E+02 ***	3.37E+01	0.61	0.07
				Intercept	4.84E+02 ***	1.38E+01		
2	0.99	0.88	0.85	log(RW)	−1.06E+02 ***	3.98E+00		
				Intercept	5.43E+02 ***	3.69E+00		

[1] AIC_1 = 1222 and Cp_1 = 1.104E+05.
[2] $+Cp_j$ is the relative contribution of each variable to Cp of the model (Equation 4).

Table 6. Regression models for the modulus of rupture (MOR_i). The models ($MOR_{1–4}$) and the model variables (X_j) are listed in order of their ranking and their contribution to the model, respectively. Minimum degrees of freedom (for MOR_2) are 123. Notations and footnotes are further explained in Table 3.

Model				Variables				
i	AIC_{rel}[1]	Cp_{rel}[1]	R^2	X_j	a_j	SE(a_j)	$\boldsymbol{a_j}$	$+Cp_j$[2]
1	1.00	1.00	0.91	ρ0	1.64E−01 ***	4.81E−03	9.58	0.98
				Q^2	−4.75E+01 ***	9.87E+00	−0.43	0.02
				Intercept	−2.25E+01 ***	2.36E+00		
2	0.90	0.53	0.84	log(RW)	−1.13E+01 ***	1.16E+00	−1.36	0.65
				LW	4.60E+01 ***	6.71E+00	0.96	0.31
				Q_t^2	−3.05E+01 **	1.13E+01	−0.24	0.04
				Intercept	4.82E+01 ***	2.74E+00		
3	0.86	0.39	0.78	log(RW)	−1.73E+01 ***	8.78E−01	−1.78	0.99
				Q_t^2	−3.60E+01 **	1.32E+01	−0.24	0.01
				Intercept	6.64E+01 ***	8.02E−01		
4	0.85	0.38	0.76	log(RW)	−1.77E+01 ***	8.86E−01		
				Intercept	6.63E+01 ***	8.22E−01		

[1] AIC_1 = 732.6 and Cp_1 = 2342.
[2] $+Cp_j$ is the relative contribution of each variable to Cp of the model (Equation 4).

distributions of bending stress (Figure 6). Figures 5A–D show that all section values decreased with AGE, independently of z_{rel}.

Discussion and conclusions

The bending stress–strain curves, σ(ε), obtained for fresh Norway spruce wood differ markedly from those for dry wood of the same species (Kollmann 1968, Märki et al. 2005), the fresh wood being more easily deformed and having a lower MOR. In terms of energy absorption of fresh wood (i.e., area under the σ(ε) curve), these two behaviors have opposite effects. A comparison of the values of energy absorption found in our study with published values for dry wood of Norway spruce undergoing bending (Kollmann 1968, Brauner et al. 2005, Märki et al. 2005) suggests that the two effects are of similar magnitude (a factor of 2). This implies that fresh and dry wood of Norway spruce absorb about the same amount of energy while bending to complete failure. Nevertheless, when analyzing the bending behavior of living tree stems, it is essential to consider the σ(ε) of fresh wood, and not of dry wood.

Most mechanical properties related to the stress–strain curve display a strong gradient in the radial direction because of the gradient in growth properties. The S-wood and the IH-wood (i.e., juvenile wood) form two distinct categories, and the OH-wood provides the transition zone. A similar radial tendency for MOE and MOR, but not for dry wood density, was also recorded by Huang et al. (2005) in logs of red cedar. Compared with S-wood, the IH-wood displays brittle failure, with about 40% lower MOR and MOE and about half of the total energy absorption per volume in bending. This means that S-wood maintains its resistance and energy absorption at

Table 7. Regression models for the modulus of elasticity (MOE_i). The models ($MOE_{1–3}$) and the model variables (X_j) are listed top down according to the ranking and contribution to the model, respectively. The minimum degrees of freedom (for MOE_1) are 124. Notations and footnotes are further explained in Table 3.

Model				Variables				
i	AIC_{rel}[1]	Cp_{rel}[1]	R^2	X_j	a_j	SE(a_j)	$\boldsymbol{a_j}$	$+Cp_j$[2]
1	1.00	1.00	0.63	log(RW)	−3.86E+03 ***	3.16E+02	−1.61	0.93
				u	−2.50E+01 ***	6.77E+00	−0.49	0.07
				Intercept	1.51E+04 ***	5.66E+02		
2	1.00	0.91	0.59	log(RW)	−3.00E+03 ***	2.08E+02		
				Intercept	1.31E+04 ***	2.24E+02		
3	0.99	0.88	0.57	log(ρ0)	1.26E+04 ***	9.72E+02		
				Intercept	−6.63E+04 ***	5.99E+03		

[1] AIC_1 = 2251 and Cp_1 = 3.642E+08.
[2] $+Cp_j$ is the relative contribution of each variable to Cp of the model (Equation 4).

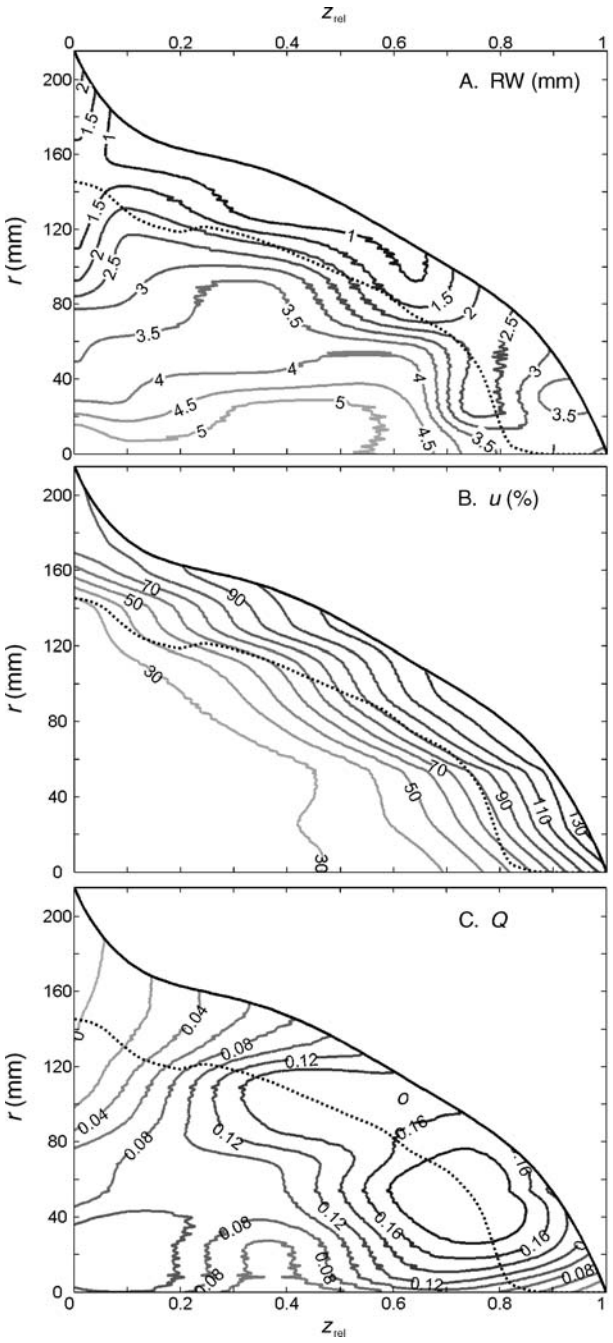

Figure 3. Three growth characteristics of the horizontal stem as functions of stem radius (r) and relative tree height (z_{rel}): (A) annual ring width (RW), (B) wood water content (u) and (C) knottiness (Q). The curved dotted line indicates the border between the heartwood and the sapwood.

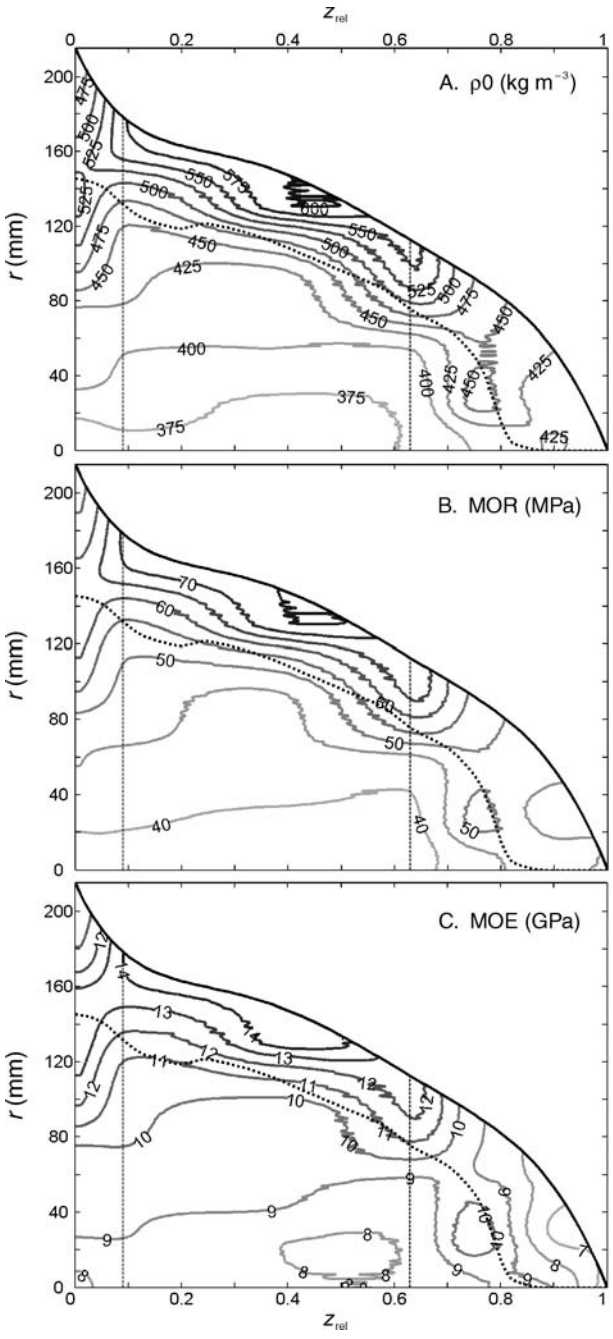

Figure 4. Three mechanical properties of the horizontal stem as a function of stem radius (r) and relative tree height (z_{rel}): (A) dry wood density (ρ0), (B) modulus of rupture (MOR) and (C) modulus of elasticity (MOE). The vertical hatched lines delimit the region for the experimentally obtained mechanical data, and the curved dotted line is the border between the heartwood and the sapwood.

strain values beyond MOR, unlike IH-wood. This difference between S-wood and IH-wood may be a result of a "global effect" found in living stems as well as in the specimens: the cross section of the bending specimen from the S-wood included 10–40 annual rings, and that of the IH-wood only 3–10 rings. The annual rings probably fail one after the other, resulting in a gradual stress redistribution, which may be more abrupt with five annual rings than with 30 rings. The phenomenon may also be associated, in part, with the lower water content of IH-wood compared with S-wood. Nevertheless, the shapes of the σ(ε)/MOR curves for IH-wood and S-wood were similar up to MOR (Figure 2B), resulting in similar idealized stress–strain curves and values of completeness, which simpli-

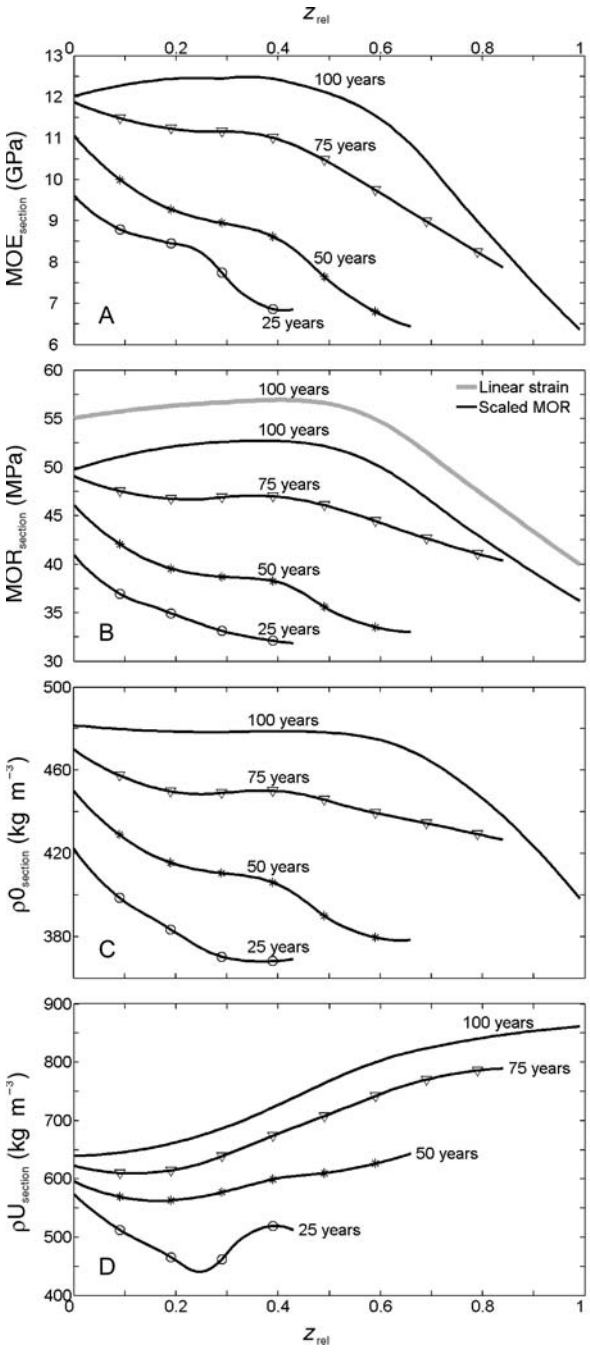

Figure 5. Four mechanical properties of the stem section as functions of relative height (z_{rel}) and cambial age at breast height (years): (A) modulus of elasticity (MOE), (B) modulus of rupture (MOR) calculated by the methods of linear strain and scaled MOR (cf. Figure 6) and (C) dry and (D) fresh wood densities (ρ0 and ρU). Panels A–D are the results from Equations 6–8, smoothed (loess algorithm) using the span = z_{rel}/3. All mechanical properties increase with age, especially MOE and MOR.

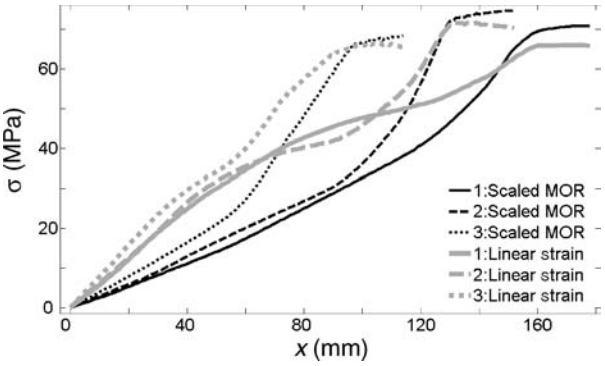

Figure 6. Bending stress (σ) as a function of the distance from pith (x), resulting from the methods based on linear strain (Equation 6) and scaled modulus of rupture (MOR) (Equation 7). Numbers 1, 2 and 3 correspond to relative tree heights 0.10, 0.37 and 0.63. The linear strain method yielded higher bending stress values than the scaled MOR method, except in the outer sapwood.

fies the computation of σ(ε) up to MOR for fresh wood at any radial position on the stem.

Dry wood density was about 40% lower in IH-wood than in S-wood. For fresh wood density, these proportions were roughly inversed because of the water content. Sapwood exhibits variations in water content during the year that can reach several tenths of a percent (Trendelenburg and Mayer-Wegelin 1955), and these variations affect the fresh wood density of the living tree stem. Our Norway spruce tree was felled in the middle of November when its water content probably approximated the mean annual water content (Schmidt-Vogt 1991). Consequently, the stem section values of fresh density should reflect the annual means.

Comparisons of the mechanical properties of the stem with the literature are relevant only if the growth conditions and properties of radial and apical growth are similar to those of the tested Norway spruce. This applied both to the values within the stem and those obtained for the stem section at cambial ages of 25, 50, 75 and 100 years at breast height. The 100-year-old co-dominant Norway spruce we studied grew in a relatively well drained soil and in competition in a fairly dense stand, and is representative of the whole study stand and of several other sites with similar climatic conditions in and around the Alps (Bräker 1981, Schweingruber 1996) and even worldwide (Core et al. 1979). It is evident that Norway spruce stems with other growth patterns, e.g., trees growing alone, on windy spots, on slopes at the tree line or that are overaged or damaged, will exhibit radial as well as cross-sectional mechanical properties that differ from the properties we observed. For example, Norway spruce trees in the Black Forest grow faster than the Norway spruce tree we investigated and exhibit between 30–40% (Trendelenburg and Mayer-Wegelin 1955) and 5–15% (Brüchert et al. 2000) lower dry wood density at equal cambial ages. For MOE, Brüchert et al. (2000) report 10–30% lower values at the same cambial age, but the MOE distribution within the stem was similar to that in our study tree. We found no published studies on MOR of fresh wood of Norway spruce combined with growth data.

The regression models help to identify growth properties having large effects on MOR, MOE and dry wood density. Our aim was to provide models for stems of a typical Norway

spruce tree. Trees growing under extreme conditions develop special stem wood properties in addition to those considered in this study such as compression wood, spiral or curly grain, callus tissue, traumatic resin ducts and gelatinous tracheids, which all influence wood mechanics (Schweingruber 1996, Mattheck 1998, Dinwoodie 2000). Previous studies have shown that age positively influences mechanical properties (e.g., Sirviö 2001). Nevertheless, old trees with large radii and widely spaced annual rings close to the bark do exist, but multivariate studies of mechanics of fresh wood of old trees are rare. We therefore decided not to present regression models including age or the radial distance from pith, although these variables slightly improved regression quality. The correlations between variables (Table 4) generally confirm previous studies (Kucera 1973, Green et al. 1999, Dinwoodie 2000). The MOE and MOR values predicted by ρ0, RW and *Q*, with a correction made for *u*, are comparable with results from previous works (Kollmann 1968, Niemz 1993, Natterer et al. 2000). If we exclude trees with special growth properties, the regression models (Tables 5–7) are likely to be generally applicable to stems of *Picea abies* L. Karst. trees.

The calculated section values of MOR, MOE and wood density (Equations 5–8) indicate that the radial and apical growth of the Norway spruce stem we studied is well designed for bending. The relatively high MOR and MOE values at the base and low values toward the top should provide several advantages for the resistance and stability of the tree, e.g., when it interacts with strong winds. A flexible upper part of the stem prevents the crown from catching wind flow, and the stem-bending resistance is highest where it is most needed, namely at the stem base, where the largest bending stresses occur. The adaptive growth observed in the radial direction of the stem economizes material in that the dense and strong wood is located close to the bark where it most effectively provides resistance and stiffness to the stem section. Although the composite equations require validation (bending of entire logs), they provide a further mechanism of how trees optimize their growth, in addition to what has been found previously (Nicoll and Ray 1996, Mattheck 1998).

The heterogeneity of wood within the stem of Norway spruce and its mechanically optimized inner structure can be accounted for using the relationships and methods presented in this contribution. The methods can be used to analyze the stability and energy dissipation of entire trees and the influence of different thinning regimes on the mechanical properties of the living stem.

Acknowledgments

The authors are indebted to the Board of the Swiss Federal Institutes of Technology for financial support, as part of the "Tree Stability and Natural Hazards" ("Naturereignisse und Baumstabilität") project. We thank Werner Gerber for his precise and successful experimental work and Silvia Dingwall for revising the text.

References

Adjanohoun, G., J.-L. Guillot, J.-D. Lanvin and R. Cholat. 1998. Small roundwood grading by non destructive X-rays and ultrasonic waves methods. 5th World Conference on Timber Engineering. Presses polytechniques et universitaires romandes, Lausanne, Switzerland. Available on the web at http://www.ndt.net/article/v04n11/adjanoh/adjanoh.htm.

Bräker, O.U. 1981. Der Alterstrend bei Jahrringdichten und Jahrringbreiten von Nadelhölzern und sein Ausgleich. Mitt. Forstl. Bundes-Versuchsanst. Wien 142:75–102.

Brauner, M., W. Weinmeister, P. Agner, S. Vospernik and B. Hoesle. 2005. Forest management decision support for evaluating forest protection effects against rockfall. For. Ecol. Manage. 207:75–85.

Brüchert, F., G. Becker and T. Speck. 2000. The mechanics of Norway spruce [*Picea abies* (L.) Karst]: mechanical properties of standing trees from different thinning regimes. For. Ecol. Manage. 135:45–62.

Core, H.A., W.A. Côté and A.C. Day. 1979. Wood: Structure and identification. 2nd Edn. Syracuse University Press, Syracuse, NY, 182 p.

Daniel, D., F.S. Wood and J.W. Gorman. 1980. Fitting equations to data: computer analysis of multifactor data. *In* Probability and Mathematical Statistics. Applied Probability and Statistics Vol. XVIII. 2nd Edn. John Wiley and sons, New York, 458 p.

Deresse, T. and R.K. Shepard. 1999. Wood properties of red pine (*Pinus resinosa* Ait.). CFRU Information Report 42, Dept. of For. Manage., University of Maine, Orono, 17 p.

DIN. 1992. Normen über Holz. Deutsches Institut für Normung. DIN-Taschenbuch Vol.31. 6th Edn. Beuth, Berlin; Köln, 260 p.

Dinwoodie, J.M. 1961. Tracheid and fibre length in timber. A review of literature. Forestry 34:125–144.

Dinwoodie, J.M. 2000. Timber: its nature and behaviour. 2nd Edn. E&FN SPON, London, 257 p.

FAO. 1998. Soil map of the world. Revised legend. World Soil Resources Report Vol. 60. FAO-UNESCO, Rome, 119 p.

Fioravanti, M. 2001. The influence of age and growth factors on microfibril angle of wood. First International Conference of European Society for Wood Mechanics, Lausanne, Switzerland, pp 47–54.

FSS. 1997. Nordic timber-grading rules. Grading rules for pine (*Pinus sylvestris*) and spruce (*Picea abies*) sawn timber. Commercial Grading Based on Evaluation of the Four Sides of Sawn Timber. 2nd Edn. Föreningen Svenska Sågverksmän (FSS)/Suomen Sahateollisuusmiesten Yhdistys (STMY)/Treindustriens Tekniske Forening (TTF), Sweden/Finland/Norway, 80 p.

Green, D.W., J.E. Winandy and D.E. Kretschmann. 1999. Mechanical properties of wood. Department of Agriculture, Forest Service, Madison, WI. Available on on the web at http://www.fpl.fs.fed.us/documnts/fplgtr/fplgtr113/ch04.pdf.

Huang, Y.S., S.S. Chen, L.L. Kuo-Huang and C.M. Lee. 2005. Growth strain in the trunk and branches of *Chamaecyparis formosensis* and its influence on tree form. Tree Physiol. 25: 1119–1126.

Ikonen, V.P., S. Kellomäki and H. Peltola. 2003. Linking tree stem properties of Scots pine (*Pinus sylvestris* L.) to sawn timber properties through simulated sawing. For. Ecol. Manage. 174:251–263.

Kollmann, F.F.P. 1968. Principles of wood science and technology. *In* Solid Wood Vol. 1. Springer-Verlag, Berlin, 592 p.

Kucera, B. 1973. Holzfehler und ihr Einfluss auf die mechanischen Eigenschaften der Fichte und Kiefer. Holztechnologie 14:8–17.

Lindstrom, H. 1996. Basic density of Norway spruce. Part II. Predicted by stem taper, mean growth ring width, and factors related to crown development. Wood Fiber Sci. 28:240–251.

Lindstrom, H. 1997. Fiber length, tracheid diameter, and latewood percentage in Norway spruce: Development from pith outwards. Wood Fiber Sci. 29:21–34.

Lundström, T., T. Jonas, V. Stöckli and W.J. Ammann. 2007. Anchorage of mature conifers: resistive turning moment, root–soil plate geometry, and orientation of root growth. Tree Physiol. 27:1217–1227.

Madsen, B. 1975. Duration of load test for wet lumber in bending. For. Prod. J. 25:33–40.

Märki, C., P. Niemz and D. Mannes. 2005. Vergleichende Untersuchungen zu ausgewählten mechanicshe Eigenschaften von EIbe und Fichte. Schweiz. Z. Forstwes. 3/4:85–91.

Mattheck, C. 1998. Design in nature: learning from trees. Springer-Verlag, Berlin, 276 p.

Milne, R. 1991. Dynamics of swaying of *Picea sitchensis*. Tree Physiol. 9:383–399.

Natterer, J. and J.L. Sandoz. 1997. Construire en bois. Notions de base. Publication IBOIS 97:16. 3rd. Edn. Reprographie Ecole polytechnique fédérale de Lausanne, Lausanne, Switzerland, 198 p.

Natterer, J., J.L. Sandoz and R. Martial. 2000. Construction en bois. Traité de Génie Civil Vol. 13. Presses Polytechniques et Universitaires Romandes, Lausanne, Switzerland, 472 p.

Neild, S.A. and C.J. Wood. 1999. Estimating stem and root-anchorage flexibility in trees. Tree Physiol. 19:141–151.

Newlin, J.A. and G.W. Trayer. 1956. Deflection of beams with special reference to shear deformations. Report 1309, U.S. Department of Agriculture, Forest Service, Madison, WI, 18 p.

Nicoll, B.C. and D. Ray. 1996. Adaptive growth of tree root systems in response to wind action and site conditions. Tree Physiol. 16: 891–898.

Niemz, P. 1993. Physik des Holzes und der Holzwerkstoffe. Holz: Anatomie, Chemie, Physik, Vol. III. DRW-Verlag, Berlin, 247 p.

Sakamoto, Y., M. Ishiguro and G. Kitagawa. 1986. Akaike information criterion statistics, Vol. XIX. KTK Scientific Publishers, Tokyo, 290 p.

Saren, M.P., R. Serimaa, S. Andersson, T. Paakkari, P. Saranpaa and E. Pesonen. 2001. Structural variation of tracheids in Norway spruce (*Picea abies* L. Karst.). J. Struct. Biol. 136:101–109.

Schmidt-Vogt, H. 1991. Die Fichte: ein Handbuch in zwei Bänden. Waldbau, Ökologie, Urwald, Wirtschaftswald, Ernährung, Düngung, Ausblick Vol. 2/3. Verlag Paul Parey, Hamburg, 781 p.

Schweingruber, F.H. 1996. Tree rings and environment. Dendroecology. Haupt Verlag, Bern, 609 p.

SIA. 2003. Timber structures—supplementary specifications. 265/1, Schweizerischer Ingenieur—und Architektenverein (SIA), Zurich, 27 p.

Siau, J.F. 1995. Wood: Influence of moisture on physical properties. Department of Wood Science and Forest Products, Virginia Polytechnic Institute and State University, Keene, NY, 227 p.

Sirviö, J. 2001. The effects of age and growth rate on wood basic density in Scots pine and Norway spruce. First International Conference of European Society for Wood Mechanics, Lausanne, Switzerland, pp 13–22.

Trendelenburg, R. and H. Mayer-Wegelin. 1955. Das Holz als Rohstoff. 2nd Edn. J.F. Lehmanns Verlag, München, 541 p.

Appendix

Table A1. List of symbols and notations and their definitions and units used in the study.

Symbol/Notation	Description	Unit
* , **, ***	Levels of significance for $P < 0.05$, $P < 0.01$ and $P < 0.001$	–
a; $\boldsymbol{a}$	Variable and intercept coefficients; standardized variable coefficient (cf. Statistical analysis)	–
AGE	Cambial age counted from pith	Years
AIC; Cp	Statistical indices of quality of regression models and variables (cf. Statistical analysis)	–
Cut	Parameter describing the annual ring curvature within the cross section of specimens (cf. Figure 1)	–
DBH	Stem diameter on bark at breast height, i.e. 1.3 m	m
E	Secant modulus of elasticity due to pure bending = σ/ε_E	MPa
ε; ε_E	Apparent bending strain (simply "bending strain"); ε without the contribution from shear deformation	–
ε_{el}; ε_{MOR}; ε_{max}	ε as σ reaches 0.4MOR (defined limit of elasticity); reaches MOR; and returns to 0.5 Mpa	–
$\varepsilon_{el\text{-}pl}$, $\alpha_{el\text{-}pl}$	The ideal elastic-ideal plastic $\sigma(\varepsilon)$-curve has a break point at $\varepsilon = \varepsilon_{el\text{-}pl}$ and $\sigma = \alpha_{el\text{-}pl}$MOR	–
F; F_{max}	Applied force when testing bending specimens; maximum applied F	N
G	Shear modulus in the z-direction, i.e. along fibers	MPa
H	Total tree height	m
η	Completeness of the material in bending (cf. Equation 3)	–
L, b, h; L_F	Length, width and height of the bending specimen; distance between support and force application	mm
LW	Late wood portion = width of late wood/RW	–
MOE; $MOE_{section}$	Modulus of elasticity = the secant modulus of $\sigma(\varepsilon)$ as 0.4MOR is reached; MOE of stem section	GPa
MOR; $MOR_{section}$	Modulus of rupture = maximum value of $\sigma(\varepsilon)$; MOR of stem section	MPa
$\int\sigma(\varepsilon)d\varepsilon$	Integration of $\sigma(\varepsilon)$ up to MOR, i.e. area under $\sigma(\varepsilon)$-curve	MPa
Q, Q_t, Q_c	Knottiness of the specimen cross-section, on the tension (t) and on the compression (c) side	–
r	The radial coordinate of the stem section, ranging from pith to bark	mm
$\rho 0$, ρU	Density of oven-dry and of fresh wood	kg m^{-3}
RW	Annual ring width	mm
σ	Bending stress	MPa
s; s_{MOR}	Mid-span deflection when testing bending specimens; s at MOR	mm
S; IH	Sapwood; inner heartwood	–
SE; R^2; P	Standard error; R-squared value of a regression; P-value of significance	–

Table A1 Con't. List of symbols and notations and their definitions and units used in the study.

Symbol/Notation	Description	Unit
τ, τ_{max}	Shear stress and resistance in the *z*-direction	MPa
u	Wood water content = mass of water/oven-dry mass	%
V	Volume of bending specimen within the bending span	m^3
W, W_{MOR}, W_{tot}	Work absorbed in bending, at MOR and at ε_{max}	N m
x, z	Cartesian coordinates of the standing tree stem: z is the height above stem base and $x = 0$ in the pith	mm, m
X; Y	Explanatory variable; response variable	–
z_{rel}	Relative height above stem base = z/H	–